J Neurophysiol 108: 2708–2716, 2012.
First published August 29, 2012; doi:10.1152/jn.00355.2012.

Motor learning reveals the existence of multiple codes for movement planning

Todd E. Hudson and Michael S. Landy
Department of Psychology and Center for Neural Science, New York University, New York, New York

Submitted 27 April 2012; accepted in final form 28 August 2012

Hudson TE, Landy MS. Motor learning reveals the existence of multiple codes for movement planning. *J Neurophysiol* 108: 2708–2716, 2012. First published August 29, 2012; doi:10.1152/jn.00355.2012.—Coordinate systems for movement planning are comprised of an anchor point (e.g., retinocentric coordinates) and a representation (encoding) of the desired movement. One of two representations is often assumed: a final-position code describing desired limb endpoint position and a vector code describing movement direction and extent. The existence of movement-planning systems using both representations is controversial. In our experiments, participants completed reaches grouped by target location (providing practice for a final-position code) and the same reaches grouped by movement vector (providing vector-code practice). Target-grouped reaches resulted in the isotropic (circular) distribution of errors predicted for position-coded reaches. The identical reaches grouped by vector resulted in error ellipses aligned with the reach direction, as predicted for vector-coded reaches. Manipulating only recent movement history to provide better learning for one or the other movement code, we provide definitive evidence that both movement representations are used in the identical task.

motor noise; motor planning; planning error; internal representation; coordinate systems

RESEARCH CONCERNING COORDINATE representations used for movement planning has focused on two aspects of that representation: codes that might be used to represent the intended movement, and the origin points used to anchor movement codes. Two movement codes are generally advocated: a vector code representing the direction and extent of the desired movement, and a position code representing desired limb position/configuration. There is clear support for vector-coded reach plans (e.g., Ghez et al. 1997; Ghilardi et al. 1995; Rosseti et al. 1995; Vindras et al. 2005). For example, the central nervous system (CNS) appears to use a vector-based code when performing slicing motions during adaptation to rotations of visual-motor space (Ghez et al. 2007; Scheidt and Ghez 2007). Consequently, most neurophysiological and computational studies of reference frames for motor control assume vector coding, focusing on possible origin-points for vector-coded movement plans (e.g., retinocentric, hand-centric, etc.: Baud-Bovy and Viviani 1998; Bernier and Grafton 2010; Ghafouri et al. 2002; Lee et al. 2011; McGuire and Sabes 2009; Pesaran et al. 2006, 2010; Thompson and Henriques 2010; van den Dobbelsteen et al. 2004). However, recent behavioral studies have reported evidence for position-coded movements (Shadmehr et al. 1993; Thaler and Todd 2009; van den Dobbelsteen et al. 2001). Studies that claim evidence for both position- and vector-coded movement planning generally use different tasks for each or use movements that allow time for feedback control, potentially confounding evidence for the code used for planning (e.g., de Grave et al. 2004; Ghez et al. 2007; Scheidt and Ghez 2007; Schenk 2006). Evidence for position-coded planning is currently only available from tasks that do not show vector-based planning, suggesting that these two movement codes might be used only in a task-dependent manner. Here, we examine the possibility that these two codes, both position and vector based, are used simultaneously when planning movements.

What might the nervous system gain from using two movement codes for planning a single movement? Since these coding schemes use different aspects of sensory feedback information to maintain their respective internal mappings, multiple codes can be combined to improve overall performance. For perceptual estimation, research indicates humans optimally combine multiple sensory cues, even partially correlated cues (Oruç et al. 2003), both within (Landy and Kojima 2001; Young et al. 1993) and across modalities (Ghahramani et al. 1997; van Beers et al. 1998), generally by a weighted average in which a cue's weight is proportional to its reliability. Similarly, there is near-optimal combination of prior and current sensory information (Tassinari et al. 2006) and reference frames (McGuire and Sabes 2009) during motor planning. We suggest that vector- and position-coded movement plans can also be combined as a weighted average at the level of the motor control signals to optimize statistical properties of the resulting multiply coded movement plan.

We test for the existence of multiple codes for movement planning by providing reach practice suitable for selective learning of the underlying representation of either a movement vector or a movement endpoint, manipulating only the presentation order of a single set of 36 reaches. Our results reveal the distinct statistical properties predicted for vector- vs. position-coded reaches in a pattern that cannot be explained by any singly coded movement planning system.

MATERIALS AND METHODS

The present study protocol was approved by the New York University Institutional Review Board. Previous work investigating the nature of the coding and coordinate systems used for movement planning has relied on manipulations of the movement task (e.g., Ghez et al. 1997; Thaler and Todd 2009) or the availability/precision of sensory inputs (e.g., McGuire and Sabes 2009), where sensory information might be varied by removing vision of the hand and/or target, blurring the target, allowing the target to be touched with the non-reaching hand, or allowing the finger to make contact with the target. Here, we take the opposite approach and maintain constant sensory inputs while manipulating the prior movement history, thereby controlling the information used to maintain internal models of the correspondence between the code for a planned movement and motor output.

Address for reprint requests and other correspondence: T. E. Hudson, New York Univ., 6 Washington Place, 8th Floor, New York, NY 10003 (e-mail: hudson@cns.nyu.edu).

Because internal representations must be maintained, we reasoned that by controlling the separation between repetitions of reaches to the same target location ("target-grouped" reaches) or reaches described by the same displacement vector ("vector-grouped" reaches), we could selectively improve/impair the precision of these representations (Verstynen and Sabes 2011). Crucially, because we were interested in isolating contributions due to the precision of internal models using these two movement codes from any fluctuation in sensory inputs, we maintained invariant sensory information in the two conditions of the experiment by presenting identical reaches during both target and vector grouping.

We test predictions of a model that combines vector- and position-coded reaches for an experiment in which subjects make speeded reaches to a 2 × 3 array of targets on a tabletop, each target surrounded by six equidistant starting points located on a circle centered on that target (Fig. 1). Subjects performed these 36 reaches in 2 groupings; each grouping consists of several blocks of reaches. One grouping (vector-grouped; Fig. 1*C*) maintains the same movement vector over many reaches to different targets within each block, whereas the second grouping (target-grouped; Fig. 1*D*) maintains the same egocentric target location over a block of many reaches from different start positions (i.e., requiring different movement vectors).

We use the fact that code-specific practice will have predictable effects on mapping precision to test for the presence of these two movement codes. Thus repeated movements to the same target where each movement uses a different vector will selectively improve a target code. Similarly, movements with the same vector, each to a different target, will selectively improve a vector code.

Movements often display anisotropic endpoint errors with the major axis of the covariance ellipse aligned with movement direction. This has been described as evidence of an underlying vector movement code (Gordon et al. 1994b). This error anisotropy makes sense for a vector-coded reach because its errors are in direction (e.g., in units of degrees) and extent (e.g., in mm). It would be highly unlikely for variability added to codes in different units to result in isotropic endpoint errors. For a position code, however, we predict errors to be isotropic (light blue circles in Fig. 2), since there is no reason to expect the representations of terminal x and y endpoint coordinates to be scaled differently within a position-coded planning system and, a priori, one would expect variability in identically scaled codes to be identical as well. Note that if error isotropy were due to execution noise, it would be present whether reaches were coded as vectors or positions, i.e., in both of our experimental conditions.

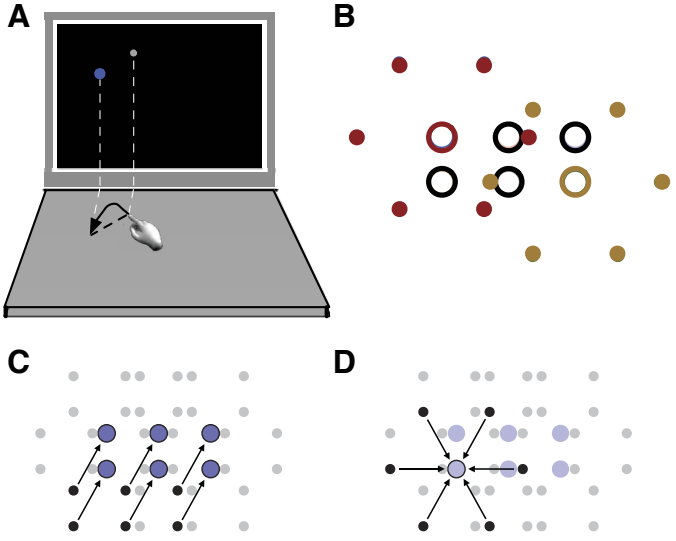

Fig. 1. Experimental apparatus and design. *A*: schematic of experimental apparatus (not to scale). Reaches were made from point-to-point on a tabletop to virtual targets that were presented on the display screen. *B*: reaches were made to targets arranged in a 3 × 2 grid (large open circles) from one of 6 start positions arranged on a circle around each target (small filled circles). For clarity only two groups of start positions, around the *top left* (red) and *bottom right* (brown) target, are shown here. *C*: full grid of target and start positions, with reaches defined by one of the 6 vectors highlighted. *D*: full grid of target and start positions, with reaches defined by one of the 6 targets highlighted. Note that the highlighted portions of *C* and *D* will be used as icons in the remaining figures to indicate when data are taken from the vector-grouped or target-grouped condition of the experiment (respectively).

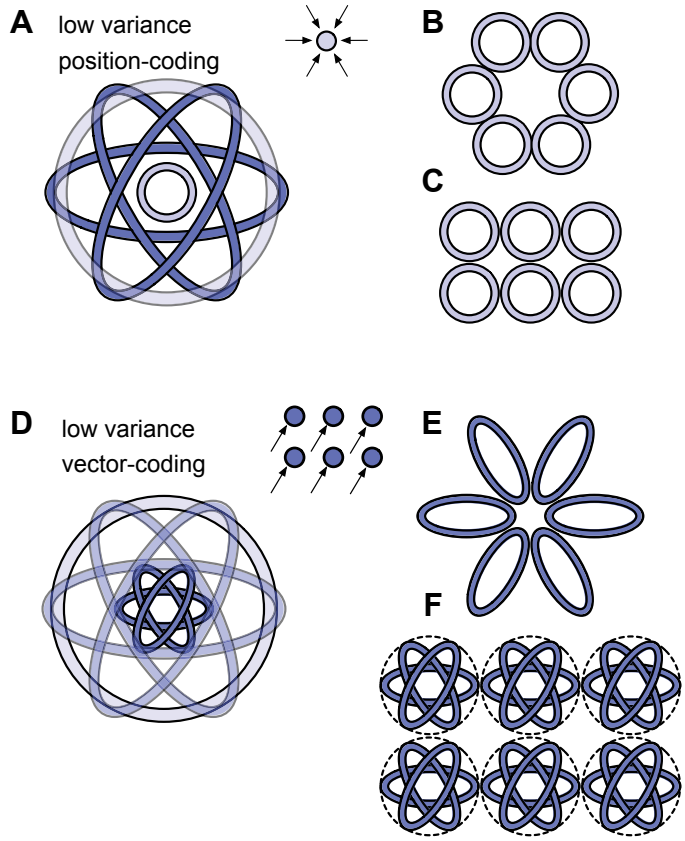

Fig. 2. Schematic representation of predicted endpoint variance during target-grouped (*A–C*; producing low-variance position coding) and vector-grouped reaches (*D–F*; producing low-variance vector coding). *A*: at the beginning of a target-grouped block, the total variance of the position- (light blue, transparent circle) and vector-coding (dark blue ellipses) systems are relatively large. After several repeated reaches to the same target, the target-coding system has improved accuracy (small light blue circle) and dominates the combined movement plan. Target-grouped reaches will display identical, small, isotropic error ellipses whether variance is computed over reaches sharing the same vector (*B*) or sharing the same target (*C*). *D*: during vector grouping, repeated reaches with the same vector improve vector-coded accuracy. Starting from the same large ellipses and circle as in *A*, the precision of the vector-coded representation improves (from transparent dark blue ellipses to smaller dark-blue ellipses, corresponding to asymptotic variance in different vector-grouped blocks) and vector coding dominates the combined movement plan. *E*: when variance is computed over reaches sharing the same vector, vector-grouped reaches will display small, anisotropic error ellipses with highest variability aligned with the movement direction. *F*: when variance is computed over vector-grouped reaches sharing the same target, variance appears larger and isotropic due to pooling over differently oriented vector-grouped ellipses.

When a new block of trials begins (start of a new vector or target), we assume that both systems begin with relatively large uncertainty (large ellipses and circles in Fig. 2*A* and *D*). By the end of a target-grouped block, the planning uncertainty of the position-coded system has decreased substantially, and similarly for the vector-coded system at the end of a vector-grouped block (small circles and small ellipses in Fig. 2, *A* and *D*, respectively). Performance (endpoint

variance or target hit rate) should improve over each block but return to baseline at the beginning of the subsequent block for both groupings. Note that if only one system is available (e.g., vector coding), these block-wise improvements of performance should not occur for the noncoded grouping. That is, if only one movement code is used there should only be improvements during the grouping that is consistent with that single encoding.

We predict that errors made during target-grouped reaches will be those of the better-practiced position-coded system and hence will be isotropic (Fig. 2, *B* and *C*), while errors made during vector-grouped reaches will be more variable along the direction of the movement (Fig. 2, *E* and *F*). This difference will be evident if variance is computed over reaches that share a common movement vector (Fig. 2, *B* and *E*). If variance is computed over reaches sharing a common target, variance will be isotropic for both conditions (Fig. 2, *C* and *F*); however, this circular covariance (computed over reaches sharing a common target) will be increased in the vector-grouped reaches (relative to the covariance computed over reaches sharing a common vector) due to the fact that for vector-grouped reaches this computation averages over multiple differently oriented ellipses (the dashed circles in Fig. 2*F* represent this isotropic variance, which pools over trials with different movement directions, each of which has anisotropic error aligned with that direction, represented by the ellipses inside the dashed circle in Fig. 2*F*). In this view, the isotropic variances for target-grouped reaches are identical whether pooled over movement direction (Fig. 2*B*) or movement target (Fig. 2*C*) because all underlying movements in target-grouped blocks have identical variance. Note that the targets we use are only a few cm apart (see *Stimuli*), so that biomechanical effects on variance should differ little across target positions.

Apparatus

Subjects were seated in a dimly lit room 42.5 cm in front of a 21-in. computer monitor, mounted to the tabletop with its center 26.5 cm above the table (Fig. 1*A*). The table extended 35.3 cm in front of the monitor. Fingertip positions were continuously monitored via two Optotrak 3020 cameras tracking six infrared light emitting diodes (IREDs) on a metal ring on the right index finger (3 IREDs on each side of the ring).

Stimuli

Subjects attempted to touch circular virtual targets on the tabletop. Virtual targets were shown in corresponding locations on a frontal computer screen (1:1 screen:actual displacement) with the screen *z*-axis (upward positive) representing the tabletop *y*-axis (forward positive); see Fig. 1*A*. Target radius was determined for each subject separately at the end of the practice phase of the experiment (see below) to produce a 0.4 hit rate for those reaches (target radii ranged from 2.6 to 6.6 mm). Presenting start, target, and feedback information onscreen while performing reaches on the tabletop does not qualitatively change the shapes of endpoint distributions (i.e., error ellipses that are elongated in the reach direction when targets are presented on the tabletop are also elongated in the reach direction when targets are presented on an upright monitor; Messier and Kalaske 1997) and prevented simultaneous view of the hand and target during a reach. Gaze monitoring of one subject under largely identical task conditions (Hudson and Landy 2012) showed no instances of looking toward the tabletop.

Experimental reaches were made to six targets, arranged as two rows of three (row spacing: 6.4 cm; column spacing: 6.8 cm). Around each of the six targets were six possible start positions at 60° intervals. Reach distance (start-target separation) was 11.75 cm in all cases (Fig. 1*B*).

Procedure

Twelve right-handed subjects performed two sets of 432 experimental reaches with the right hand, one set grouped according to reach vector and one set grouped according to reach target. Six subjects performed vector-grouped reaches before target-grouped reaches; the remaining six performed the reach groupings in reverse order. Before each set of experimental reaches, subjects made a small number of practice reaches (75 before the first set and 25 before the second set) that had neither a target nor a vector grouping (no targets or vectors were repeated and no targets or vectors corresponded to those of experimental reaches). This allowed us to obtain a measure of overall variance and set the size of the target disc so that it would be approximately equally difficult to hit for all subjects.

All reaches. All reaches proceeded as follows: subjects brought their right index finger to the start position as cued by a visual indication of the start and current fingertip position, triggering the start of the trial. At this point the start position, the indicator of the current fingertip position and the target and endpoint position feedback from the previous trial were removed. Next, the target was displayed, followed 50 ms later by a brief tone indicating that subjects could begin the reach when ready. Movement onset was defined as the moment the fingertip moved outside of a bounding radius of 4 mm from the start position; the movement was required to be completed (i.e., the fingertip lifted from and then retouched the tabletop) within 300 ms of movement onset; too-slow reaches were repeated at the end of the block (where a block comprises the sequence of reaches to a single target or corresponding to a single vector). The endpoint of the reach was defined as the point at which the fingertip fell below a 3-mm height from the tabletop and fingertip velocity fell below 0.75 mm/s. The location of the fingertip at the end of the movement was displayed as a static red dot, and online fingertip feedback (white dot, 2 mm diam) reappeared for the next reach when the fingertip had come within 5 cm of the next start position.

Experimental reaches. Experimental reaches were broken into two sets: vector- and target-grouped reaches. Each grouping consisted of 12 repetitions of the 36 start-position/target combinations (864 total reaches). Subjects were given the identical 36 reaches in both sets; the only difference was the order in which they were given. Vector-grouped reaches kept the vector that defined the desired reach trajectory and distance constant for a block comprising all 12 repetitions of all 6 different reaches defined by that vector (chosen in random order), and then another of the 6 vectors was chosen at random and all reaches corresponding to that vector were completed, until all 6 vectors had been accounted for. Similarly, target-grouped reaches kept the target position constant for a block of 72 trials (reaches chosen in random order), followed by a block corresponding to a different target position and so on for six blocks. All six blocks of target- and vector-grouped reaches flowed seamlessly into one another without break or other notification that a new block had begun.

Because target radius was not constant across subjects, the visual indication of the target was always given as a blue dot (2-mm radius) at the target center, regardless of actual target radius. The target exploded visually to indicate when it was touched, i.e., when the location on the tabletop corresponding to the target was touched.

Practice reaches. Start and target positions were chosen so that no reach vectors or targets were repeated, no experimental reach vectors or targets were used, and reach distances were drawn from a uniform distribution (5-cm wide) centered on the experimental reach distance. These reaches were designed to allow a measurement of overall variance without providing practice of experimental reaches. Reaches that were too slow were repeated, and thus the practice session also served to teach participants the time limit. Reaches that were too slow were not included in the variance computation (nor were too-slow trials used in the analysis of experimental reaches). Reach targets could not be touched during practice (the effective target radius was

0), and subjects were simply instructed to touch as close as possible to the target dot.

Data Collection

Before each experimental session, subjects (fitted with IREDs) touched their right index finger (pointing finger) to a metal calibration nub located to the right of the screen while the Optotrak recorded the locations of the six IREDs on the finger 150 times. The best linear transformations converting three vectors derived from the three IREDs on each side of the ring (each defining a coordinate frame) into the fingertip location at the metal nub were computed (Hudson et al. 2010). This allowed us to precisely locate the fingertip, as opposed to simply the IREDs, in space. During each reach, we recorded the three-dimensional positions of the IREDs at 200 Hz and converted them into fingertip location using this transformation. Tangential reach velocity was defined as the ratio of distance traveled between consecutive data samples to the time elapsed between samples in the direction of the reach. Instantaneous reach direction was estimated as the arctangent of the vector connecting the previous to the current datum.

RESULTS

Reach Trajectories and Hit Rates

We first note that changes observed in reach trajectories and endpoints during vector- and target-grouped reaches were almost entirely restricted to movement variance, rather than in mean observed trajectory. Mean trajectories are plotted in Fig. 3*A* for the two groupings. Mean trajectories overlap so completely that the two groupings are plotted separately to allow both to be seen. We summarize fingertip positional variance by "equivalent standard deviation," which we define as the standard deviation of a circular covariance with the same area as a given covariance ellipse (i.e., as $\sqrt{A/\pi}$, where A is the area of the covariance ellipse). The change in fingertip equivalent standard deviation over the course of the reach is plotted in Fig. 3*B* for the two conditions (collapsing across subject and reach direction). Both curves have the shape of a square root function. The shapes of these functions suggest that all reaches were relatively straight, containing no online corrections (which would have produced data with an inverted "U" shape). There were slight, nonsignificant differences in mean tangential velocities in the two conditions (Fig. 3*C*). All plots in Fig. 3 are computed after first normalizing the duration of each reach to 1 and binning position or velocity data according to the proportion of the reach that had been completed. Total reach duration was not significantly different between vector- and target-grouped reaches (*t*-test, $P > 0.05$). Thus accuracy differences between the two conditions are not due to speed-accuracy tradeoff.

We see no evidence of course correction or online feedback control in these reaches. This is not surprising given that reaches were fast (averaging 268 ms) and gaze was directed at the display that showed the starting point and target; thus subjects had only a peripheral view of the hand in the dimly lit experiment room. Consistent with this lack of feedback control, average spatial trajectories were nearly straight, with no hint of the terminal "hook" that is observed when course adjustments are implemented late in a reach. Average velocity profiles have a single peak, also giving no indication of late course corrections. Such corrections and corresponding dual-peaked velocity profiles are seen in longer-duration reaches, e.g., in the data of Scheidt et al. (2005) in which reaches lasted between 400 and 500 ms. In addition, average initial and final reach direction (i.e., instantaneous direction averaged over the first or second halves of the movement, computed relative to the straight line joining start and target positions) are significantly correlated in both conditions of the current experiment.

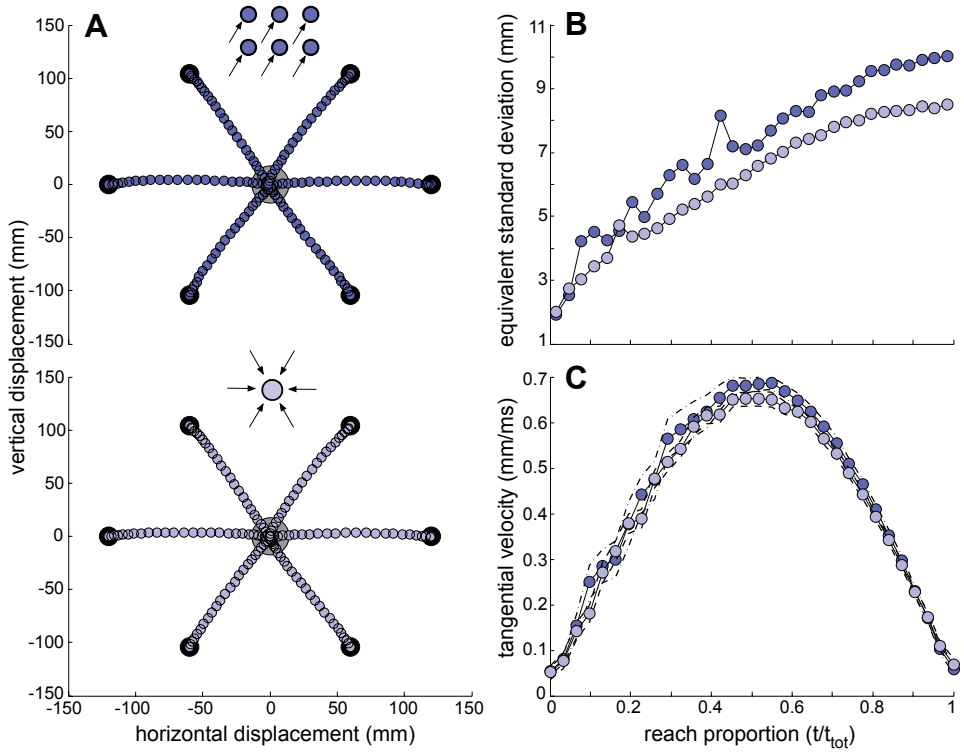

Fig. 3. Average reach kinematics. *A*: fingertip position in the horizontal plane while reaching in each of the six directions. Reaches are presented relative to the target position, which is plotted at the origin. Vector-grouped (dark blue) and target-grouped (light blue) reaches are plotted on separate axes because the averages overlap to such an extent that only one grouping would be discernable if plotted together. *B*: fingertip equivalent SD (i.e., $\sqrt{A/\pi}$, where A is the area of the covariance ellipse of *x*-*y* fingertip position) as a function of the proportion of total reach duration that has elapsed for vector-grouped (dark blue) or target-grouped (light blue) reaches. First, fingertip positions were binned according to proportion of reach time elapsed. SDs were then computed from those positions, collapsing across reach direction and averaging across subjects, to produce one curve for each of the two experimental conditions. *C*: fingertip velocity as a function of the proportion of total reach duration that has elapsed for vector-grouped (dark blue) or target-grouped (light blue) reaches. Error curves indicate ± 1 SE of the mean velocity across subjects in each condition (dashed: vector-grouped; dash-dotted: target-grouped).

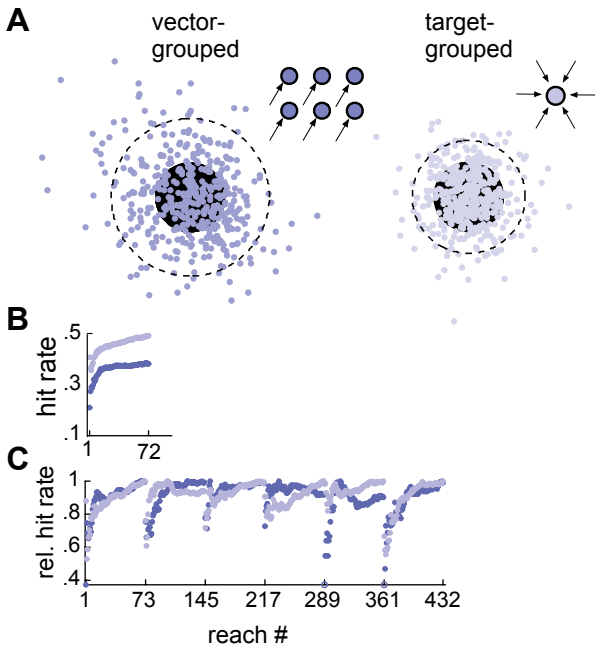

Fig. 4. Reach endpoints and hit rates. *A*: reach endpoints from one subject. Endpoints (blue dots) are plotted relative to the target (filled black circle) for vector-grouped reaches on the left, and target-grouped reaches on the right. Dashed black circles show 1 SD of the best-fit pooled circular error variance. *B*: running averages of hit rates computed from the beginning of each block of target-grouped (light blue) and vector-grouped (dark blue) reaches. Data combined across all subjects and blocks. *C*: running averages of hit rates from single targets (target-grouped) and vectors (vector-grouped), normalized to 1 at the peak hit rate within each block (absolute average hit rates are shown in *B*). Open circles indicate data points below the plot, which occurs at the first datum within the fifth and last vector (hit rates were 0.27 and 0.0, respectively).

Correlations were computed across reaches and averaged across subjects (vector grouped: $r = 0.49$; target grouped: $r = 0.50$; $P < 0.05$ in both cases). The fact that these correlations are identical suggests that any differences between the two conditions result from differences in planning rather than a difference between conditions of online control during reach execution.

Figure 4*A* shows individual target-relative reach endpoints for one subject, demonstrating the overall variance difference (visible even in single subjects) produced by grouping reaches based on targets vs. vectors: target grouping led to substantially smaller endpoint variance [paired *t*-test of equivalent standard deviations: $t(11) = 2.7$; $P < 0.05$].

Cumulative hit rates within a vector- or target-grouped block of reaches are shown in Fig. 4*B* (pooled over subjects and blocks). Figure 4*C* shows cumulative hit rates computed from the start of each block of same-target or same-vector reaches (averaged across subjects). These hit rates conform to our predictions: hit rates improve regardless of block as seen in the initial rise in hit rates in all traces and demonstrate the predicted transient performance decrement at the beginning of each block in both groupings. The overall hit rate is higher for target-grouped reaches due to the lower endpoint variance in that condition.

Pattern of Observed Covariances

Our primary predictions concern the covariance structures of errors observed under target- vs. vector-grouped reaches. As has been suggested previously, we predict a vector-based movement code will result in anisotropic reach errors (Gordon et al. 1994b), whereas we predict spatially isotropic errors resulting from position-coded reaches. We report covariances of reach errors relative to the mean endpoint for each target within each block of 72 reaches. Thus, for target-grouped reaches, the error for each reach is relative to the mean of those 72 reaches (and then these reach errors are pooled across subjects and possibly across common vectors in other blocks). For vector-grouped reaches, the error for each reach is computed relative to the mean endpoint for the 12 reaches in that block toward the same target, and then errors are pooled across blocks and subjects. For the target-grouped condition, one might instead compute reach errors relative to the mean endpoint in each block of the 12 repetitions of a single target-vector combination before pooling. This alternative method of pooling the data for computing covariances does not change any of our conclusions.

Figures 5 and 6 present covariance ellipses from vector- and position-grouped reach endpoints. Each ellipse in Fig. 5*A* is computed from vector-grouped reaches from all reaches with the same movement vector (i.e., each ellipse corresponds to one block of reaches, where the ellipse at the right was computed from the block of leftward reach vectors, etc.). Each ellipse in Fig. 5*B* was computed from target-grouped reaches, based on all reaches to the same target (one block of reaches per target; ellipses arranged spatially according to the corresponding target location). The pattern of covariance ellipse shapes is as predicted (Fig. 2, *C* and *E*): ellipses computed from vector-grouped reaches are anisotropic and elongated in the direction of the reach (Fig. 5*A*), whereas reaches computed from target-grouped reaches are isotropic (Fig. 5*B*).

Figure 5 presents error ellipses for reach endpoints pooled as they were experienced during the experiment, by target for

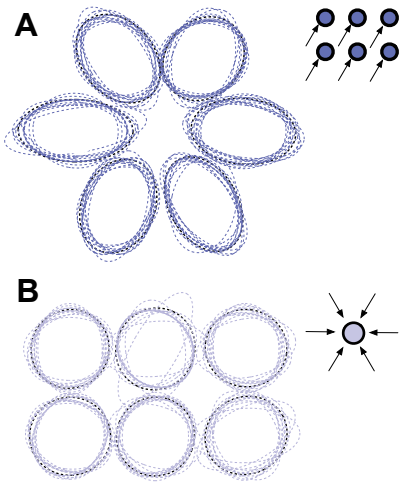

Fig. 5. Covariance ellipses selected by grouping. *A*: ellipses computed from vector-grouped data. Each ellipse corresponds to one reach vector (the 0° ellipse corresponds to reaches in the 180° reach direction, etc.). Equivalent SD: 9.7 mm. *B*: ellipses for data grouped according to the target position (each ellipse positioned according to the target location in the 3 × 2 array). Equivalent SD: 8.7 mm. Ellipses are normalized to unit area to emphasize ellipse shapes. Note that the area of a circular covariance is $\sigma^2\pi$ mm^2, where σ is the equivalent SD. Colored ellipses correspond to one target/vector per subject; black ellipses are computed across subjects.

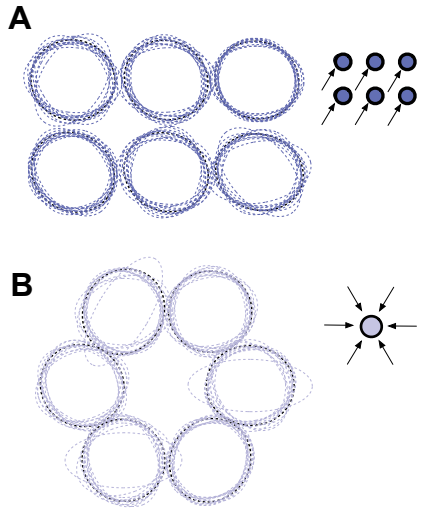

Fig. 6. Covariance ellipses computed according to "opposite grouping." *A*: covariance ellipses from vector-grouped data (also used for Fig. 5A), but pooled by target position, regardless of reach vector. Equivalent SD: 10.4 mm. *B*: covariance ellipses from target-grouped data (also used for Fig. 5*B*), pooled by reach vector regardless of target location. Equivalent SD: 8.8 mm. Ellipses are again normalized to unit area for plotting.

target-grouped reaches and by vector for vector-grouped reaches. However, it is always possible to pool reach endpoints both by target and by vector, regardless of the experienced grouping. Figure 6 presents error ellipses based on the same data but pooled differently. Here, vector-grouped reaches are pooled according to target (Fig. 6*A*), and target-grouped reaches are separated by vector (Fig. 6*B*). None of the ellipses in Fig. 6 show any indication of reliably elongated shape, consistent with our predictions (Fig. 2, *B* and *F*). Thus, when position-coded planning dominates the output (during target grouping), reach endpoint variance is isotropic even when pooled over reaches with identical vector (Fig. 6*B*). The area of the average ellipse in Fig. 6*A* is significantly larger than the average ellipses in Fig. 5, *A* and *B* [$t(11) = 2.9$ and 3.2, respectively; both $P < 0.01$]. Again, the comparison with Fig. 5*A* is consistent with our predictions, as our theory suggests the ellipses in Fig. 6*A* involve pooling over ellipses with different orientations (Fig. 2*F*), resulting in larger variance that is only apparently circular (hiding the underlying anisotropic variances from each constituent vector). The area of the average ellipse in Fig. 6*B* is not significantly different than the area of the average ellipse in Fig. 5*B* but is significantly smaller than the average ellipses in Figs. 5*A* and 6*A* [$t(11) = 2.3$ and 3.1, respectively; both $P < 0.05$]. These results are consistent with our predictions (Fig. 2, *B* and *C*) and also suggest that the asymptotic performance of the position code is superior to that of the vector code, under the conditions of these experiments. Hit-rate data (Fig. 4) also show better asymptotic performance for target- than for vector-grouped reaches. Although our theory does not require that asymptotic variance be larger in either vector- or position-coded reaches, we note that this finding (smaller asymptotic position-coded variance) can explain the inference drawn from several previous studies that reaches are more likely to be coded in terms of position than as a vector.

The ellipses presented in Figs. 5 and 6 display the general pattern predicted in Fig. 2. To quantitatively compare observed covariances to those predicted in Fig. 2, we plot histograms of ellipse orientation (Fig. 7*A*) and a measure of elongation (the ratio of variances along and perpendicular to the reach direction; Fig. 7*B*) for the two critical covariance computations of the experiment: the vector-grouped data separated by vector (as in Fig. 5*A*), and the target-grouped data separated by vector (as in Fig. 6*B*). For the vector-grouped condition, histograms of the major axes of covariance ellipses form clearly separated clusters around their respective reach directions (Fig. 7*A*, plotted above the axis). On the other hand, the major axes for target-grouped reaches are uniformly distributed (Fig. 7*A*, plotted below the axis), as expected for random variation in

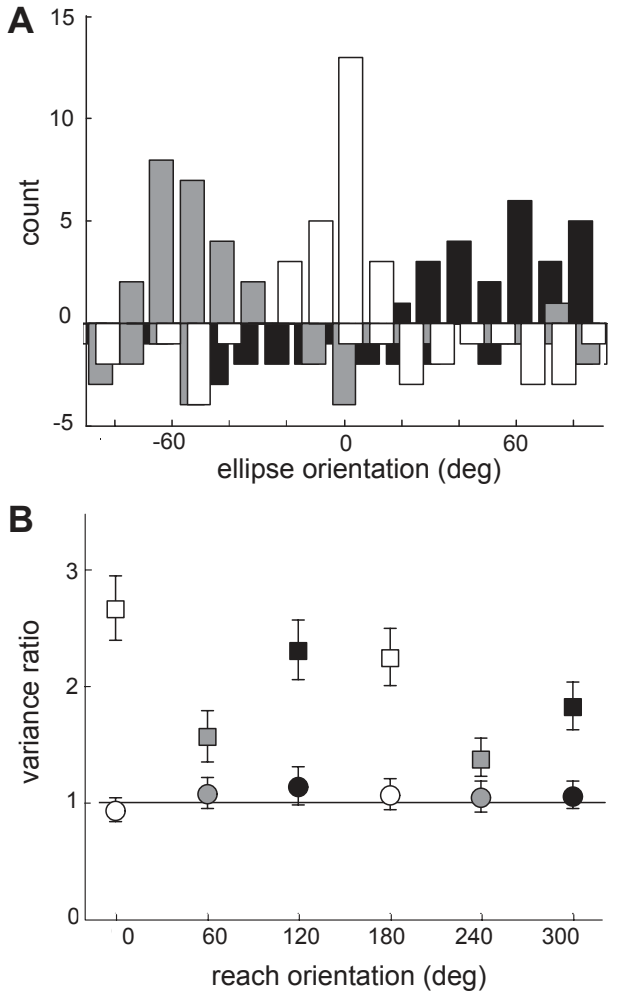

Fig. 7. Comparison of theoretical predictions to data. *A*: histograms of ellipse orientation for each reach direction (−60°/+120°, 0°/180°, and 60°/−120° in grey, white and black bars, respectively). Histograms corresponding to vector-grouped data (pooled by vector) are plotted above the axis. Target-grouped data (also pooled by vector) are plotted below the axis. *B*: ratio of variances (parallel/perpendicular to the reach direction) derived from the two conditions of the experiment. Reach directions are color-coded as in *A*. Vector-coded reaches (squares) produce elongated error ellipses (ratio > 1), whereas target-coded reaches (circles) are predicted to produce circular error distributions (ratio = 1). Error bars indicate the 95% confidence interval. Average ratio in the vector-grouped condition was 1.98 ± 0.09 and was 1.03 ± 0.05 in the target-grouped condition. In both plots, only the two critical cases (vector-grouped data organized by vector, and target-grouped data reorganized by vector) are shown.

isotropic data. Figure 7*B* tests the prediction that vector-grouped ellipses will be elongated in the reach direction, while target-grouped ellipses in the grouped-by-vector arrangement are predicted to be nearly isotropic. For an isotropic covariance matrix, the two variance components are equal (i.e., their ratio is 1). The data conform closely to this prediction. For the target-grouped condition, all variance ratios are indistinguishable from unity (circles; *t*-tests comparing ratios across subjects, all $P > 0.05$), while all vector-grouped ratios are significantly greater than unity (squares; all $P < 0.05$).

The overall pattern of results matches the predictions of a model in which movements are planned using two different codes: vector-based and target-based. The vector-based code leads to error ellipses elongated along the direction of the movement while the target-based code does not. van Beers et al. (1998) argued that anisotropic endpoint errors are due to execution noise. In that study, the identical movement was repeated many times, arguably reducing movement-planning-related variability. This may have led to the dominance of execution noise they inferred, which they proposed was due to the target/arm configuration and reach speed. However, in the current study neither target/arm configurations nor average reach kinematics changed between the two experimental conditions. Therefore, we must conclude that it is a difference in movement planning, not execution noise, that led to our results.

DISCUSSION

The internal representation used to code movement plans is a central theme of motor neuroscience, with a growing consensus that reach plans are coded not simply as a movement vector (Gordon et al. 1994a,b; Krakauer et al. 2000; Vindras and Viviani 2002) or desired position (Thaler and Todd 2009; van den Dobbelsteen et al. 2001), but using multiple codes, position and vector based, the relative contributions of which to the final movement depend on the circumstances of the reach (Scheidt and Ghez 2007). Initial indications of multiple movement codes focused on showing that predictable changes in movement output result from altered sensory inputs or from different motor tasks (Ghez et al. 2007; Scheidt and Ghez 2007; Thaler and Todd 2010). Here, we demonstrate distinct statistical properties predicted for these two subsystems via changes in the precision of sensory-motor mappings, while keeping the task, biomechanics, and sensory inputs constant. The fact that we show evidence of both vector- and position-based movement plans in the identical reaches, coupled with the fact that our experiments involved only natural unperturbed reaches, provides strong evidence for the theory that multiply coded reach plans are the norm during everyday movements.

Multiple vs. Single Movement Codes

One could cherry pick our results to argue for either single movement code. For example, overall variances and hit rates suggest that a single position code is most consistent with our results. Target grouping, which provides the best practice for a position code, produced the lowest-variance pooled error ellipses (Fig. 4*A*) and highest hit rates (Fig. 4*B*). Indeed, the transition from target- to vector-grouped reaches coincided with a substantial performance decrement, even though in this ordering vector-grouped reaches do not begin until >400 trials of "practice" with the same reaches (i.e., the target-grouped reaches). This seems paradoxical given the general expectation that practice improves performance but makes sense if reaches are coded as desired endpoints. However, other aspects of our results are consistent with vector-coded movement plans, such as the elongated covariance ellipses oriented to reach vectors observed in Fig. 5*A*. When pooled across reach directions (Fig. 6*B*), one would also predict that vector-coded reaches produce circular covariance ellipses; pooling errors across the differently oriented ellipses in Fig. 5*A* from vector-coded reaches toward a given target would be isotropic (Fig. 2*F*).

Only when taking account of the full set of findings can we conclusively rule out both single-coding mechanisms in favor of a multiply coded movement-planning model. If the CNS coded all reaches as vectors, pooling target-grouped errors by vector should exhibit their putative underlying vector coding. This is not what we find. Instead, we see isotropic error ellipses in Fig. 6*B*, the equivalent standard deviation of which is the same as those in Fig. 5*B*. This pattern appears possible only from multiply coded control signals. Multiply coded signals predict both high-variance isotropic errors in Fig. 6*A* (relative to Fig. 5*A*) due to the superposition of underlying low-variance vector-coded reaches (Fig. 2*F*) and also predict isotropic errors in Fig. 6*B* (with equivalent standard deviation equal to those in Fig. 5*B*) from an underlying low-variance position code (Fig. 2*B*).

Anisotropy of Error Variance

Figure 2 also suggests an explanation of the pattern of pooled variances (Fig. 4*A*), hit rates (Fig. 4, *B* and *C*), and error ellipse areas (Figs. 5 and 6). The predicted relative sizes of variance ellipses following target-grouped practice are shown in Fig. 2*A*. Based on the optimal combination rule (DeGroot 1970), the resulting motor command signals should favor position-coded movement plans following target-grouped practice. This would result in isotropic errors, regardless of whether one pools errors from those target-grouped reaches by vector (Fig. 2*B*) or by target (Fig. 2*C*).

The predicted relative sizes of position- and vector-coded variance ellipses following vector-grouped reach practice are shown in Fig. 2*D*. Motor command signals should favor vector-coded inputs under this grouping. Command signals with naturally anisotropic uncertainty will be revealed when reach endpoints are pooled by vector but hidden in the superposition when reaches are pooled by target. Further, this superposition predicts exaggerated endpoint variance when pooling over differently oriented elliptical error distributions, consistent with the observed variance in Fig. 4*A*, *left*.

In addition to the above, we note that these results bear on a second issue pertaining to the anisotropy of reach endpoints. Previously, the fact that endpoint errors have been found elongated in the reach direction has been interpreted, as here, in terms of the uncertainty of the underlying encoding. A second interpretation has previously been possible: anisotropic endpoint errors could simply reflect a signal-dependent noise component present in all motor commands (Harris and Wolpert 1998). We show that signal-dependent noise alone cannot account for error distributions that are elongated in the direction of the reach, because this would require that all reaches, including those grouped by target, display elongated errors

when pooled by reach direction and a larger-area isotropic superposition when pooled by target.

Transformation vs. Planning Noise

In addition to planning noise, reach endpoints in these experiments should contain a noise component due to the transformation necessary to use target and feedback information presented on an upright monitor to reach from point to point on the tabletop, i.e., transformation noise. The experimental results of Messier and Kalaska (1997) are relevant to this point. Their experiments directly compare tabletop and monitor presentation of targets for point-to-point reaches on a tabletop. Their tabletop-presentation condition (with 1:1 scaling of seen and actual target distances) used a method known to produce elongated error ellipses (van Beers et al. 2004) and indeed replicated the well-known finding that errors are elongated in the reach direction. Then, using the same method except that targets were presented on an upright monitor as here, they found that errors, although increased overall, were again elongated in the reach direction; indeed, they found no differences between variance ratios (along vs. perpendicular to the reach direction) for their two presentation types.

Although Messier and Kalaska (1997) imposed a 1:2.4 scaling of monitor to tabletop distances, which would tend to enhance the contribution of transformation noise relative to what would be expected from the 1:1 scaling used here, they found that the qualitative shapes of error ellipses were unchanged by the addition of transformation noise. That is, errors were always larger along the reach direction. Thus, even if participants in our experiment had learned the monitor-to-tabletop transformation somewhat better for one or the other condition, or for some blocks of trials relative to others, a difference in the amount of transformation noise would not have changed the qualitative patterns of errors seen in our results. Even if our participants were somehow able to completely eliminate transformation noise in some subset of our conditions or blocks, this would not produce a qualitative change in ellipse shape, because even when transformation noise is completely absent, as in the tabletop condition of Messier and Kalaska (1997), it does not change the qualitative shapes of error ellipses relative to their monitor-presentation results. Therefore, we conclude that the pattern of results found in the present study is due to learning in the planning of movements, not in the transformation from display to tabletop.

How Are Multiple Codes Combined?

If these two subsystems are always in operation and contributing to individual reaches, then the question arises: what is the nature of motor commands sent to arm motor units resulting from multiple codes? There appear to be two possibilities, although they cannot be discriminated based on the current data.

One suggestion (Ghez et al. 2007 Scheidt and Ghez 2007) is that the initial portion of a reach primarily involves vector-based motor torques that direct the arm along a trajectory with an initial force profile consistent with a given reach magnitude, whereas the final portion of the reach primarily involves matching muscle-tension and cutaneous variables to position-coded values. If the two movement codes were connected to the initial and final portions of a reach in this way, one could predict the current results by supposing, depending on recent reach history, that more or less weight is given to the initial or final portion of the reach in terms of its contribution to the overall movement. For example, if there were no reliable information relevant to the reach endpoint as such, the full reach trajectory would be determined by vector-based commands. Similarly, when only target-position information is available, the "final" matching of desired sensory parameters to position-coded values would begin at reach initiation.

It also appears possible that movement signals are combined at the level of motor units. Here, we must assume that both codes are responsible for a full movement plan and do not simply code an initial or final phase of the reach. If movement plans derived from both codes are sent as weighted sets of motor-unit activation strengths, the resulting movement would again be a weighted average of the two reach plans. Of course, there are several possible variations: for example, the initial and final phases of reach plans derived from the two codes could be differentially weighted much as the weights of different visual cues change through the course of a reach (Greenwald et al. 2005). This would mimic the proposal above that early reach variables are vector-coded whereas reach termination is position coded, because relative weightings would switch from favoring vector-coded to position-coded reach plans in the early and late phases of the reach, respectively.

Summary

We provide evidence showing that both target- and position-coded movement plans are used in planning the identical reaches. Simultaneous planning in multiple coordinate systems allows movement plans to be combined to produce statistically optimal movements within the biological constraints imposed by neural computation noise, biomechanics, etc. Given the advantages of planning movements in multiple coordinate systems, and the fact that we find evidence for the use of multiple coordinate systems in unperturbed reaches, we propose that multiply-coded movements are the norm rather than something elicited only in the laboratory by unusual movement tasks, task-specific control of sensory feedback, or movements constrained by specialized robotic manipulanda. This has far-reaching implications for studying the neurophysiology of movement-related coordinate systems, which currently focus only on vector-coded movement plans.

Our results also have important implications for rehabilitation following stroke, as recent evidence suggests that motor deficits secondary to stroke can selectively impair endpoint or trajectory planning (e.g., Haaland 2004). Rehabilitative strategies designed to improve motor performance should focus on training regimes tailored to the corresponding movement code, just as our experiments selectively train one movement planning system or the other by presenting movement series optimized for forming internal representations using each of the two movement codes separately.

GRANTS

This work was supported by National Eye Institute Grant EY-08266.

DISCLOSURES

No conflicts of interest, financial or otherwise, are declared by the author(s).

AUTHOR CONTRIBUTIONS

Author contributions: T.E.H. and M.S.L. conception and design of research; T.E.H. performed experiments; T.E.H. analyzed data; T.E.H. interpreted results of experiments; T.E.H. prepared figures; T.E.H. drafted manuscript; T.E.H. and M.S.L. edited and revised manuscript; T.E.H. and M.S.L. approved final version of manuscript.

REFERENCES

Baud-Bovy G, Viviani P. Pointing to kinesthetic targets in space. *J Neurosci* 18: 1528–1545, 1998.

Bernier PM, Grafton ST. Human posterior parietal cortex flexibly determines reference frames for reaching based on sensory context. *Neuron* 68: 776–788, 2010.

de Grave DD, Brenner E, Smeets JB. Illusions as a tool to study the coding of pointing movements. *Exp Brain Res* 155: 56–62, 2004.

DeGroot M. *Optimal Statistical Decisions*. New York: McGraw-Hill, 1970.

Ghafouri M, Archambault PS, Adamovich SV, Feldman AG. Pointing movements may be produced in different frames of reference depending on the task demand. *Brain Res* 929: 117–128, 2002.

Ghahramani Z, Wolpert DM, Jordan MI. Computational models of sensorimotor integraiton. In: *Self-Organization, Comptational Maps and Motor Control*, edited by Morasso PG, Sanguineti V. Amsterdam: North-Holland, 1997, p. 117–147.

Ghez C, Favilla M, Ghilardi MF, Gordon J, Bermejo R, Pullman S. Discrete and continuous planning of hand movements and isometric force trajectories. *Exp Brain Res* 115: 217–233, 1997.

Ghez C, Scheidt R, Heijink H. Different learned coordinate frames for planning trajectories and final positions in reaching. *J Neurophysiol* 98: 3614–3626, 2007.

Ghilardi MF, Gordon J, Ghez C. Learning a visuomotor transformation in a local area of work space produces directional biases in other areas. *J Neurophysiol* 73: 2535–2539, 1995.

Gordon J, Ghilardi MF, Cooper SE, Ghez C. Accuracy of planar reaching movements. II. Systematic extent errors resulting from inertial anisotropy. *Exp Brain Res* 99: 112–130, 1994a.

Gordon J, Ghilardi MF, Ghez C. Accuracy of planar reaching movements. I. Independence of direction and extent variability. *Exp Brain Res* 99: 97–111, 1994b.

Greenwald HS, Knill DC, Saunders JA. Integrating visual cues for motor control: a matter of time. *Vision Res* 45: 1975–1989, 2005.

Haaland KY, Prestopnik JL, Knight RT, Lee RR. Hemispheric asymmetries for kinematic and positional aspects of reaching. *Brain* 127: 1145–1158, 2004.

Harris CM, Wolpert DM. Signal-dependent noise determines motor planning. *Nature* 394: 780–784, 1998.

Hudson TE, Landy MS. Measuring adaptation with a sinusoidal perturbation function. *J Neurosci Methods* 208: 48–58, 2012.

Hudson TE, Tassinari H, Landy MS. Compensation for changing motor uncertainty. *PLoS Comput Biol* 6: e1000982, 2010.

Krakauer JW, Pine ZM, Ghilardi MF, Ghez C. Learning of visuomotor transformations for vectorial planning of reaching trajectories. *J Neurosci* 20: 8916–8924, 2000.

Landy MS, Kojima H. Ideal cue combination for localizing texture-defined edges. *J Opt Soc Am A Opt Image Sci Vis* 18: 2307–2320, 2001.

Lee B, Pesaran B, Andersen RA. Area MSTd neurons encode visual stimuli in eye coordinates during fixation and pursuit. *J Neurophysiol* 105: 60–68, 2011.

McGuire LM, Sabes PN. Sensory transformations and the use of multiple reference frames for reach planning. *Nat Neurosci* 12: 1056–1061, 2009.

Messier J, Kalaska JF. Differential effect of task conditions on errors of direction and extent of reaching movements. *Exp Brain Res* 115: 469–478, 1997.

Oruç I, Maloney LT, Landy MS. Weighted linear cue combination with possibly correlated error. *Vision Res* 43: 2451–2468, 2003.

Pesaran B, Nelson MJ, Andersen RA. A relative position code for saccades in dorsal premotor cortex. *J Neurosci* 30: 6527–6537, 2010.

Pesaran B, Nelson MJ, Andersen RA. Dorsal premotor neurons encode the relative position of the hand, eye, and goal during reach planning. *Neuron* 51: 125–134, 2006.

Rossetti Y, Desmurget M, Prablanc C. Vectorial coding of movement: vision, proprioception, or both? *J Neurophysiol* 74: 457–463, 1995.

Scheidt RA, Conditt MA, Secco EL, Mussa-Ivaldi FA. Interaction of visual and proprioceptive feedback during adaptation of human reaching *J Neurophysiol* 93: 3200–3213, 2005.

Scheidt RA, Ghez C. Separate adaptive mechanisms for controlling trajectory and final position in reaching. *J Neurophysiol* 98: 3600–3613, 2007.

Schenk T. An allocentric rather than perceptual deficit in patient D.F. *Nat Neurosci* 9: 1369–1370, 2006.

Shadmehr R, Mussa-Ivaldi FA, Bizzi E. Postural force fields of the human arm and their role in generating multijoint movements. *J Neurosci* 13: 45–62, 1993.

Tassinari H, Hudson TE, Landy MS. Combining priors and noisy visual cues in a rapid pointing task. *J Neurosci* 26: 10154–10163, 2006.

Thaler L, Todd JT. Evidence from visuomotor adaptation for two partially independent visuomotor systems. *J Exp Psychol Hum Percept Perform* 36: 924–935, 2010.

Thaler L, Todd JT. The control parameters used by the CNS to guide the hand depend on the visuo-motor task: evidence from visually guided pointing. *Neuroscience* 159: 578–598, 2009.

Thompson AA, Henriques DY. Locations of serial reach targets are coded in multiple reference frames. *Vision Res* 50: 2651–2660, 2010.

van Beers RJ, Haggard P, Wolpert DM. The role of execution noise in movement variability. *J Neurophysiol* 91: 1050–1063, 2004.

van Beers RJ, Sittig AC, Denier van der Gon JJ. The precision of proprioceptive position sense. *Exp Brain Res* 122: 367–377, 1998.

van den Dobbelsteen JJ, Brenner E, Smeets JB. Body-centered visuomotor adaptation. *J Neurophysiol* 92: 416–423, 2004.

van den Dobbelsteen JJ, Brenner E, Smeets JB. Endpoints of arm movements to visual targets. *Exp Brain Res* 138: 279–287, 2001.

Verstynen T, Sabes PN. How each movement changes the next: an experimental and theoretical study of fast adaptive priors in reaching. *J Neurosci* 31: 10050–10059, 2011.

Vindras P, Desmurget M, Viviani P. Error parsing in visuomotor pointing reveals independent processing of amplitude and direction. *J Neurophysiol* 94: 1212–1224, 2005.

Vindras P, Viviani P. Altering the visuomotor gain. Evidence that motor plans deal with vector quantities. *Exp Brain Res* 147: 280–295, 2002.

Young MJ, Landy MS, Maloney LT. A perturbation analysis of depth perception from combinations of texture and motion cues. *Vision Res* 33: 2685–2696, 1993.